

Near-Optimal Coding for Massive Multiple Access

Kuan Hsieh
University of Cambridge, UK
kh525@cam.ac.uk

Cynthia Rush
Columbia University, USA
cynthia.rush@columbia.edu

Ramji Venkataramanan
University of Cambridge, UK
ramji.v@eng.cam.ac.uk

Abstract—We study the Gaussian multiple access channel (MAC) in the asymptotic regime where the number of users grows linearly with the codelength. We analyze coding schemes based on random linear models with approximate message passing (AMP) decoding. For fixed target error rate and number of bits per user, we obtain the exact tradeoff between energy-per-bit and the user density achievable in the large system limit. We show that a spatially coupled coding scheme with AMP decoding achieves near-optimal tradeoff for a large range of user densities. We also study the spectral efficiency versus energy-per-bit tradeoff in the regime where the number of bits per user is large.

I. INTRODUCTION

Consider the L -user Gaussian multiple access channel (MAC), where the output $\mathbf{y} \in \mathbb{R}^n$ is generated as

$$\mathbf{y} = \sum_{\ell=1}^L \mathbf{c}_\ell + \mathbf{w}, \quad (1)$$

where $\mathbf{c}_\ell \in \mathbb{R}^n$ is the codeword of user $\ell \in [L]$, and the noise vector $\mathbf{w} \in \mathbb{R}^n$ has i.i.d. Gaussian entries $w_i \sim \mathcal{N}(0, \sigma^2)$.

We consider the Gaussian MAC in the asymptotic regime proposed by Polyanskiy et al. [1], [2] where 1) the number of users L grows linearly with the codelength n , i.e., $L = \mu n$ for some fixed user density μ , and 2) the number of bits transmitted by each user (per-user payload) is fixed and independent of n . (Throughout the paper, “asymptotic” refers to the large system limit where L and n both tend to infinity with μ held constant.) In this regime, we wish to understand the optimal tradeoffs between the user density μ , the per-user payload, the probability of error, and the signal-to-noise ratio $\frac{E_b}{N_0}$. Here E_b is the energy-per-bit and $N_0 = 2\sigma^2$ is the noise spectral density. We also wish to construct efficient coding schemes whose performance approaches the optimal tradeoffs.

Decoding performance is measured via the user error rate (UER):

$$\text{UER} = \frac{1}{L} \sum_{\ell=1}^L \mathbb{1} \{ \hat{\mathbf{x}}_\ell \neq \mathbf{x}_\ell \}, \quad (2)$$

where \mathbf{x}_ℓ denotes the message sent by user ℓ , and $\hat{\mathbf{x}}_\ell$ is the decoder’s estimate of the message. The *per-user probability of error* (PUPE) error criterion used in [1], [2] is the expected value of the UER. In [1], [2], the authors obtained converse and achievability bounds on the minimum $\frac{E_b}{N_0}$ required to achieve a decoding error of PUPE $\leq \epsilon$ for a given $\epsilon > 0$, when the user density μ and user payload are fixed. The achievability bound was based on the coding scheme where users encode

their messages with i.i.d. Gaussian codebooks, and messages are decoded with (joint) maximum likelihood (ML) decoding.

In this paper, we analyze coding schemes based on random linear models with approximate message passing (AMP) decoding. We derive the exact asymptotic achievability regions of these schemes, and find that the asymptotic achievability of a coding scheme based on *spatially coupled* Gaussian matrices and AMP decoding nearly matches the converse bound for a large range of user densities. To the best of our knowledge, this is the first efficient coding scheme to do so in this MAC regime. The spatially coupled scheme can be interpreted as generalized time-sharing: the coupling structure specifies which users are active during each channel use. We also analyze the performance of these coding schemes as the user payload grows large.

Related works: The recent papers [3], [4] study the fundamental tradeoffs in the quasi-static fading MAC in the proportional scaling regime. A number of works [5]–[7] have studied MACs under different scaling regimes, energy constraints and error criteria. We emphasize that our problem setting is distinct from random access [1], [5], [8] and from unsourced multiple access [1], [9], [10]. (In the Gaussian MAC, the users have different codebooks and can all be simultaneously active.) The AMP algorithms used for decoding in this paper are similar to the ones proposed for random linear models and sparse superposition codes [11]–[14].

II. RANDOM LINEAR CODING AND AMP DECODING

We consider coding schemes where the codewords of user $\ell \in [L]$ are constructed as $\mathbf{c}_\ell = \mathbf{A}_\ell \mathbf{x}_\ell$, where $\mathbf{A}_\ell \in \mathbb{R}^{n \times B}$ is a random matrix and $\mathbf{x}_\ell \in \mathbb{R}^B$ encodes the message of user ℓ . In this coding framework, the channel model (1) can be written as

$$\mathbf{y} = \mathbf{A} \mathbf{x} + \mathbf{w}, \quad (3)$$

where the *design matrix* $\mathbf{A} \in \mathbb{R}^{n \times LB}$ is the (horizontal) concatenation of matrices $\mathbf{A}_1, \dots, \mathbf{A}_L$, and the *message vector* $\mathbf{x} \in \mathbb{R}^{LB}$ is the concatenation of vectors $\mathbf{x}_1, \dots, \mathbf{x}_L$. We will assume that the squared norm of each column of \mathbf{A} equals 1 in expectation.

The L sections of \mathbf{x} (which each correspond to a user’s message) are drawn i.i.d. from $p_{\mathbf{X}_{\text{sec}}}$, which is a probability mass function over a finite set of length B vectors. The per-user payload is therefore equal to the entropy $H(\mathbf{X}_{\text{sec}})$, where $\mathbf{X}_{\text{sec}} \sim p_{\mathbf{X}_{\text{sec}}}$. The codeword energy constraint is denoted by E , i.e., we require $p_{\mathbf{X}_{\text{sec}}}$ to satisfy $\mathbb{E} \|\mathbf{X}_{\text{sec}}\|^2 = E < \infty$.

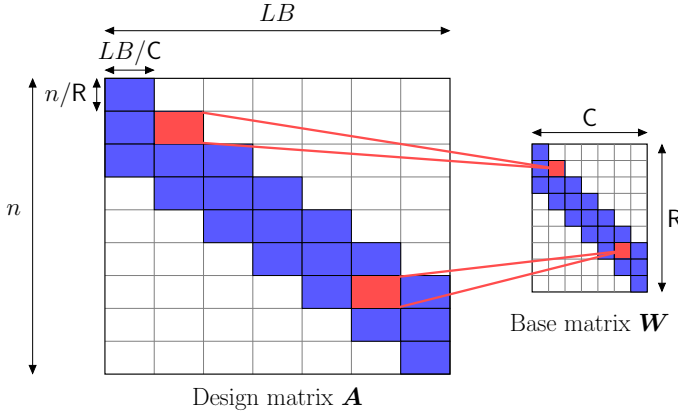


Fig. 1. Spatially coupled design matrix \mathbf{A} defined using an $(\omega = 3, \Lambda = 7, \rho = 0)$ base matrix \mathbf{W} . Each square in \mathbf{W} represents a scalar entry that specifies the variance of the entries in a block of \mathbf{A} . The white parts of \mathbf{A} and \mathbf{W} correspond to zeros.

Example 2.1 (Random codebooks): Let $p_{\mathbf{X}_{\text{sec}}}$ be the distribution over length B vectors that chooses uniformly at random one of its entries to be non-zero, taking the value \sqrt{E} . This corresponds to a per-user payload of $\log_2 B$ bits. Then, if the entries of the design matrix \mathbf{A} are i.i.d. $\mathcal{N}(0, \frac{1}{n})$, in the coding scheme each user selects one-of- B random codewords of expected energy $\mathbb{E}\|c_\ell\|^2 = E = E_b \log_2 B$. In the rest of the paper, we denote the choice of $p_{\mathbf{X}_{\text{sec}}}$ used in this example by p_1 .

Example 2.2 (Random codebooks with binary modulation): Let $p_{\mathbf{X}_{\text{sec}}}$ be the distribution over length B vectors that chooses uniformly at random one of its B entries to be non-zero, taking values in $\{\pm\sqrt{E}\}$ with equal probability. This corresponds to a per-user payload of $1 + \log_2 B$ bits. Then, if the entries of the design matrix \mathbf{A} are i.i.d. $\mathcal{N}(0, \frac{1}{n})$, in the coding scheme each user encodes $\log_2 B$ bits in the selection of one-of- B random codewords, and an additional 1 bit in whether to flip the sign of the codeword. When $B = 1$, this coding scheme corresponds to random code division multiple access (CDMA) with antipodal signalling.

A. Spatially Coupled Coding Schemes

A spatially coupled (Gaussian) design matrix $\mathbf{A} \in \mathbb{R}^{n \times LB}$ is divided into R -by- C equally size blocks. The entries within each block are i.i.d. Gaussian with zero mean and variance specified by the corresponding entry of a base matrix $\mathbf{W} \in \mathbb{R}_+^{R \times C}$. The design matrix \mathbf{A} is constructed by replacing each entry of the base matrix W_{rc} , by an $\frac{n}{R} \times \frac{LB}{C}$ matrix with entries drawn i.i.d. from $\mathcal{N}(0, \frac{W_{rc}}{n/R})$. See Fig. 1 for an example. Hence, the design matrix \mathbf{A} has independent Gaussian entries

$$A_{ij} \sim \mathcal{N}\left(0, \frac{1}{n/R} W_{r(i)c(j)}\right), \quad \text{for } i \in [n], j \in [LB]. \quad (4)$$

The operators $r(\cdot) : [n] \rightarrow [R]$ and $c(\cdot) : [LB] \rightarrow [C]$ in (4) map a particular row or column index to its corresponding row block or column block index. We require C to divide L , resulting in $L/C \geq 1$ sections per column block.

The entries of the base matrix \mathbf{W} must satisfy $\sum_{r=1}^R W_{rc} = 1$ for $c \in [C]$ to ensure that the columns of the design matrix \mathbf{A} have unit norm in expectation. The trivial base matrix with $R = C = 1$ (single entry equal to 1) corresponds to the design matrix with i.i.d. $\mathcal{N}(0, \frac{1}{n})$ entries. In this paper we will consider a class of base matrices called (ω, Λ, ρ) base matrices [14], [15].

Definition 2.1: An (ω, Λ, ρ) base matrix \mathbf{W} is described by three parameters: coupling width $\omega \geq 1$, coupling length $\Lambda \geq 2\omega - 1$, and $\rho \in [0, 1)$ which specifies the fraction of “energy” allocated to the uncoupled entries in each column. The matrix has $R = \Lambda + \omega - 1$ rows and $C = \Lambda$ columns, with each column having ω identical non-zero entries in the band-diagonal. The (r, c) th entry of the base matrix, for $r \in [R], c \in [C]$, is given by

$$W_{rc} = \begin{cases} \frac{1-\rho}{\omega} & \text{if } c \leq r \leq c + \omega - 1, \\ \frac{\rho}{\Lambda - 1} & \text{otherwise.} \end{cases} \quad (5)$$

When $\rho = 0$, as in Fig. 1, the base matrix has non-zero entries only in the band-diagonal part. For example, the base matrix in Fig. 1 has parameters $(\omega = 3, \Lambda = 7, \rho = 0)$.

Each entry of the base matrix corresponds to an $\frac{n}{R} \times \frac{LB}{C}$ block of the design matrix \mathbf{A} , and each block can be viewed as an (uncoupled) i.i.d. Gaussian design matrix with $\frac{L}{C}$ sections, code length $\frac{n}{R}$, and user density

$$\mu_{\text{inner}} = \frac{L/C}{n/R} = \frac{R}{C} \mu = \left(1 + \frac{\omega - 1}{\Lambda}\right) \mu. \quad (6)$$

Since $\omega > 1$ in spatially coupled systems, we have $\mu < \mu_{\text{inner}}$. This difference is often referred to as a “rate loss” in the literature of spatially coupled error correcting codes [15]–[18], and becomes negligible when Λ is much larger than ω .

The spatially coupled coding scheme can be viewed as *block-wise time-division with overlap*. Consider a scenario with $L = 35$ users, $n = 45$ channel uses, and a spatially coupled design matrix constructed using the base matrix $\mathbf{W} \in \mathbb{R}_+^{9 \times 7}$ in Fig. 1. Each block of the design matrix corresponds to 5 channel uses and 5 users. Assuming each channel use corresponds to one time instant, users in the first column block (users 1 to 5) will transmit during time instants 1 to 15 (corresponding to the first $\omega = 3$ row blocks); users 6 to 10 will transmit during time instants 6 to 20, and so on.

B. AMP Decoding and State Evolution

We consider an efficient AMP decoder that aims to reconstruct the message vector \mathbf{x} from the channel output \mathbf{y} . The design matrix \mathbf{A} , the base matrix \mathbf{W} , the distribution $p_{\mathbf{X}_{\text{sec}}}$, and the channel noise variance σ^2 are known. AMP algorithms have been proposed for estimation in the random linear model (3) with spatially coupled design matrices \mathbf{A} [11]–[14]. The AMP decoder iteratively produces message vector estimates $\mathbf{x}^t \in \mathbb{R}^{LB}$ for iterations $t = 1, 2, \dots$ as follows. Initialize \mathbf{x}^0 to the all-zero vector, and for $t \geq 0$, iteratively compute:

$$\begin{aligned} \mathbf{z}^t &= \mathbf{y} - \mathbf{A}\mathbf{x}^t + \tilde{\mathbf{v}}^t \odot \mathbf{z}^{t-1}, \\ \mathbf{x}^{t+1} &= \eta^t(\mathbf{x}^t + (\tilde{\mathbf{S}}^t \odot \mathbf{A})^* \mathbf{z}^t). \end{aligned} \quad (7)$$

Here \odot is the Hadamard (entry-wise) product and quantities with negative iteration indices are set to zero. The vector $\tilde{\mathbf{v}}^t \in \mathbb{R}^n$ and the matrix $\tilde{\mathbf{S}} \in \mathbb{R}^{n \times LB}$ will be described in terms of the following state evolution parameters.

The performance of the AMP in the large system limit is succinctly captured by a deterministic recursion called *state evolution*. State evolution iteratively defines vectors $\gamma^t, \phi^t \in \mathbb{R}^R$ and $\tau^t, \psi^t \in \mathbb{R}^C$ as follows. Initialize $\psi_c^0 = E$ for $\mathbf{c} \in [\mathbf{C}]$, and for $t \geq 0$, iteratively compute:

$$\gamma_r^t = \sum_{\mathbf{c}=1}^{\mathbf{C}} W_{rc} \psi_{\mathbf{c}}^t, \quad \phi_r^t = \sigma^2 + \mu_{\text{inner}} \gamma_r^t, \quad r \in [\mathbf{R}], \quad (8)$$

$$\tau_{\mathbf{c}}^t = \left[\sum_{r=1}^{\mathbf{R}} \frac{W_{rc}}{\phi_r^t} \right]^{-1}, \quad \psi_{\mathbf{c}}^{t+1} = \text{mmse}(1/\tau_{\mathbf{c}}^t), \quad \mathbf{c} \in [\mathbf{C}], \quad (9)$$

where $\mu_{\text{inner}} = \frac{\mathbf{R}}{\mathbf{C}} \mu$ from (6), and

$$\begin{aligned} \text{mmse}(1/\tau) &= \mathbb{E} \left\| \mathbf{X}_{\text{sec}} - \mathbb{E} \left[\mathbf{X}_{\text{sec}} \mid \mathbf{X}_{\text{sec}} + \sqrt{\tau} \mathbf{Z} \right] \right\|^2 \\ &\stackrel{(i)}{=} E \left[1 - \mathbb{E} \left[\frac{e^{\sqrt{\frac{E}{\tau}} Z_1}}{e^{\sqrt{\frac{E}{\tau}} Z_1} + e^{-E/\tau} \sum_{j=2}^B e^{\sqrt{\frac{E}{\tau}} Z_j}} \right] \right], \end{aligned} \quad (10)$$

where $\mathbf{X}_{\text{sec}} \sim p_{\mathbf{X}_{\text{sec}}}$ and $\mathbf{Z} = [Z_1, \dots, Z_B]$ is a standard Gaussian vector independent of \mathbf{X}_{sec} . The equality (i) holds when $\mathbf{X}_{\text{sec}} \sim p_1$, where p_1 is described in Example 2.1.

The vector $\tilde{\mathbf{v}}^t \in \mathbb{R}^n$ and the matrix $\tilde{\mathbf{S}}^t \in \mathbb{R}^{n \times LB}$ in (7) both have a block-wise structure and are defined using state evolution parameters as follows. For $i \in [n]$ and $j \in [LB]$,

$$\tilde{v}_i^t = \frac{\mu_{\text{inner}} \gamma_{r(i)}^t}{\phi_{r(i)}^{t-1}}, \quad \tilde{S}_{ij}^t = \frac{\tau_{\mathbf{c}(j)}^t}{\phi_{r(i)}^t}, \quad (11)$$

where we recall that $r(i)$ and $\mathbf{c}(j)$ denote the row and column block index of the i th row entry and j th column entry, respectively. The vector $\tilde{\mathbf{v}}^0$ is defined to be all-zeros.

In each iteration, the AMP decoder (7) produces an effective observation $\mathbf{s}^t = \mathbf{x}^t + (\tilde{\mathbf{S}}^t \odot \mathbf{A})^* \mathbf{z}^t$, which has the following approximate representation: for an index j in column block \mathbf{c} of the message vector \mathbf{x} , we have $s_j^t \approx x_j + \sqrt{\tau_{\mathbf{c}}^t} Z_j$, where $\{Z_j\} \sim_{\text{i.i.d.}} \mathcal{N}(0, 1)$. The estimate \mathbf{x}^{t+1} in (7) is then the minimum mean square error (MMSE) estimate of \mathbf{x} given \mathbf{s}^t , computed using the assumed distribution. This leads to the following definition of the denoising function $\eta^t = (\eta_1^t, \dots, \eta_{LB}^t)$ in (7): for index j in section $\ell \in [L]$, which we denote by $j \in \text{sec}(\ell)$,

$$\eta_j^t(\mathbf{s}) = \mathbb{E} \left[(\mathbf{X}_{\text{sec}})_j \mid \mathbf{X}_{\text{sec}} + \sqrt{\tau_{\mathbf{c}(j)}^t} \mathbf{Z} = \mathbf{s}_\ell \right] \quad (12)$$

$$\stackrel{(i)}{=} \sqrt{E} \cdot \frac{\exp\left(\frac{s_j \sqrt{E}}{\tau_{\mathbf{c}(j)}^t}\right)}{\sum_{i \in \text{sec}(\ell)} \exp\left(\frac{s_i \sqrt{E}}{\tau_{\mathbf{c}(j)}^t}\right)}, \quad (13)$$

where we recall that the ℓ th section of a vector $\mathbf{s} \in \mathbb{R}^{LB}$ is denoted by $\mathbf{s}_\ell \in \mathbb{R}^B$. The equality (i) holds when $\mathbf{X}_{\text{sec}} \sim p_1$.

In addition, the decoder can also produce a *hard-decision* maximum a posteriori (MAP) estimate from \mathbf{s}^t , which we

denote by $\hat{\mathbf{x}}^{t+1}$. For section ℓ in column block $\mathbf{c} \in [\mathbf{C}]$, the ℓ th section of this hard-decision estimate is given by

$$\hat{\mathbf{x}}_\ell^{t+1} = \arg \max_{\mathbf{x}' \in \mathcal{S}} \mathbb{P} \left(\mathbf{X}_{\text{sec}} = \mathbf{x}' \mid \mathbf{X}_{\text{sec}} + \sqrt{\tau_{\mathbf{c}}^t} \mathbf{Z} = \mathbf{s}_\ell^t \right), \quad (14)$$

where \mathcal{S} is the support of $p_{\mathbf{X}_{\text{sec}}}$. When $\mathbf{X}_{\text{sec}} \sim p_1$, index $j \in \text{sec}(\ell)$ of this hard-decision estimate is given by

$$\hat{x}_j^{t+1} = \begin{cases} \sqrt{E} & \text{if } s_j^t > s_i^t \text{ for all } i \in \text{sec}(\ell) \setminus j, \\ 0 & \text{otherwise.} \end{cases} \quad (15)$$

For the special case where the entries of the design matrix \mathbf{A} are i.i.d. $\mathcal{N}(0, \frac{1}{n})$, the AMP decoder (7) and the state evolution (8)–(9) can be simplified. The AMP decoder initializes the message vector estimate \mathbf{x}^0 to the all-zero vector, and for $t \geq 0$, iteratively computes:

$$\begin{aligned} \mathbf{z}^t &= \mathbf{y} - \mathbf{A} \mathbf{x}^t + \frac{\mu \psi^t}{\tau^{t-1}} \mathbf{z}^{t-1}, \\ \mathbf{x}^{t+1} &= \eta^t(\mathbf{x}^t + \mathbf{A}^* \mathbf{z}^t), \end{aligned} \quad (16)$$

where quantities with negative iteration indices are set to zero. The scalars τ^t and ψ^t are given by the state evolution. The state evolution initializes $\psi^0 = E$, and for $t \geq 0$, iteratively computes:

$$\begin{aligned} \tau^t &= \sigma^2 + \mu \psi^t, \\ \psi^{t+1} &= \text{mmse}(1/\tau^t), \end{aligned} \quad (17)$$

where the mmse function is defined in (10). Furthermore, when the design matrix has i.i.d. Gaussian entries, the denoising function η^t in (12) and the hard-decision estimate $\hat{\mathbf{x}}^{t+1}$ in (14) are defined using the state evolution parameter τ^t as the Gaussian noise variance.

III. ASYMPTOTIC UER ACHIEVED BY AMP DECODING

We now characterize the asymptotic user error rate (see (2)) achieved by coding schemes based on i.i.d. and spatially coupled Gaussian design matrices with AMP decoding. These results are stated in terms of a *potential function*.

Potential function: Consider the single-section Gaussian channel with noise variance τ :

$$\mathbf{S}_\tau = \mathbf{X}_{\text{sec}} + \sqrt{\tau} \mathbf{Z}, \quad (18)$$

where $\mathbf{X}_{\text{sec}} \sim p_{\mathbf{X}_{\text{sec}}}$ and $\mathbf{Z} \in \mathbb{R}^B$ is a standard Gaussian vector independent of \mathbf{X}_{sec} . The potential function for the random linear system (3) with user density $\mu = \frac{L}{n}$ and channel noise variance σ^2 is defined as

$$\mathcal{F}(\mu, \sigma^2, \psi) = I(\mathbf{X}_{\text{sec}}; \mathbf{S}_\tau) + \frac{1}{2\mu} \left[\ln \left(\frac{\tau}{\sigma^2} \right) - \frac{\mu \psi}{\tau} \right], \quad (19)$$

where $\psi \in [0, E]$, $\tau = \sigma^2 + \mu \psi$, and the mutual information $I(\mathbf{X}_{\text{sec}}; \mathbf{S}_\tau)$ is computed using the channel (18). If $\mathbf{X}_{\text{sec}} \sim p_1$ and $\mathbf{Z} = [Z_1, \dots, Z_B]$, then

$$I(\mathbf{X}_{\text{sec}}; \mathbf{S}_\tau) = \frac{E}{\tau} + \ln B - \mathbb{E} \ln \left[e^{\frac{E}{\tau} + \sqrt{\frac{E}{\tau}} Z_1} + \sum_{j=2}^B e^{\sqrt{\frac{E}{\tau}} Z_j} \right].$$

Define the set of potential function minimizers (w.r.t. ψ) as:

$$\mathcal{M}(\mu, \sigma^2) = \left\{ \arg \min_{\psi \in [0, E]} \mathcal{F}(\mu, \sigma^2, \psi) \right\}. \quad (20)$$

Consider decoding \mathbf{X}_{sec} in the Gaussian channel in (18). The MMSE decoder $\hat{\mathbf{x}}_{\text{sec}}^{\text{MMSE}}(\mathbf{S}_\tau) = \mathbb{E}[\mathbf{X}_{\text{sec}} | \mathbf{S}_\tau]$, achieves the MMSE given by (10). The MAP decoder $\hat{\mathbf{x}}_{\text{sec}}^{\text{MAP}}(\mathbf{S}_\tau) = \arg \max_{\mathbf{x}'} \mathbb{P}(\mathbf{X}_{\text{sec}} = \mathbf{x}' | \mathbf{S}_\tau)$, achieves the minimum probability of error, given by

$$P_e(\tau) = \mathbb{P}(\hat{\mathbf{x}}_{\text{sec}}^{\text{MAP}}(\mathbf{S}_\tau) \neq \mathbf{X}_{\text{sec}}) \quad (21)$$

$$\stackrel{(i)}{=} 1 - \mathbb{E} \left[\Phi \left(\sqrt{E/\tau} + Z \right)^{B-1} \right]. \quad (22)$$

where $Z \sim \mathcal{N}(0, 1)$ and $\Phi(\cdot)$ is the distribution function of the standard normal. The equality (i) holds when $\mathbf{X}_{\text{sec}} \sim p_1$.

Theorem 1 (i.i.d. Gaussian matrices with AMP decoding): Consider the linear model (3), with the entries of the design matrix \mathbf{A} i.i.d. $\sim \mathcal{N}(0, \frac{1}{n})$ and the L sections of the message vector \mathbf{x} i.i.d. $\sim p_{\mathbf{X}_{\text{sec}}}$. Let $\hat{\mathbf{x}}^t$ be the AMP hard-decision estimate of \mathbf{x} after iteration t (defined in (14)), and recall that τ^t, ψ^t are outputs of the state evolution (17).

1) The sequences $\{\tau^t\}_{t \geq 0}$ and $\{\psi^t\}_{t \geq 0}$ are non-increasing and converge to fixed points $\tau^{\text{FP}}, \psi^{\text{FP}}$, where

$$\tau^{\text{FP}} := \sigma^2 + \mu\psi^{\text{FP}}, \quad (23)$$

$$\begin{aligned} \psi^{\text{FP}} &:= \max \left\{ \psi : \psi = \text{mmse} \left(\frac{1}{\sigma^2 + \mu\psi} \right) \right\} \\ &= \max \left\{ \psi : \frac{\partial \mathcal{F}(\mu, \sigma^2, \psi)}{\partial \psi} = 0 \right\}. \end{aligned} \quad (24)$$

The potential function $\mathcal{F}(\mu, \sigma^2, \psi)$ is defined in (19).

2) Fix $\delta > 0$, and let T denote the first iteration for which $\tau^t \leq \tau^{\text{FP}} + \delta$. Then the user error rate of the AMP decoder after $T + 1$ iterations satisfies

$$\lim_{L \rightarrow \infty} \frac{1}{L} \sum_{\ell=1}^L \mathbb{1}\{\hat{\mathbf{x}}_\ell^{T+1} \neq \mathbf{x}_\ell\} \stackrel{\text{a.s.}}{=} P_e(\tau^T) \leq P_e(\tau^{\text{FP}} + \delta), \quad (25)$$

where the limit is taken with $\frac{L}{n} = \mu$ held constant and $P_e(\cdot)$ is defined in (21).

Proof: 1) We first prove that the sequence $\{\psi^t\}_{t \geq 0}$ is non-increasing and converges to the fixed point ψ^{FP} defined in (24). Then the result that $\{\tau^t\}_{t \geq 0}$ is non-increasing and converges to $\tau^{\text{FP}} = \sigma^2 + \mu\psi^{\text{FP}}$ immediately follows since $\tau^t = \sigma^2 + \mu\psi^t$ (an increasing function of ψ^t).

Let us consider the state evolution (17) as a single recursion:

$$\psi^{t+1} = \text{mmse}((\sigma^2 + \mu\psi^t)^{-1}). \quad (26)$$

Starting from $\psi^0 = \mathbb{E}\|\mathbf{X}_{\text{sec}}\|^2 = E$, we have that

$$\psi^1 = \text{mmse}((\sigma^2 + \mu E)^{-1}) \leq E = \psi^0, \quad (27)$$

where the inequality is because the trivial all zero estimate of a random section \mathbf{X}_{sec} achieves an expected squared error of E . The mmse function defined in (10) is a non-increasing function of its argument snr – this has been rigorously shown in [19], [20]. Since its argument $\text{snr} = (\sigma^2 + \mu\psi^t)^{-1}$ is

decreasing in ψ^t , the mmse function is non-decreasing in ψ^t . Therefore, if $\psi^t \leq \psi^{t-1}$, then

$$\psi^{t+1} = \text{mmse}((\sigma^2 + \mu\psi^t)^{-1}) \leq \text{mmse}((\sigma^2 + \mu\psi^{t-1})^{-1}) = \psi^t,$$

which together with (27) shows that the sequence $\{\psi^t\}_{t \geq 0}$ is non-increasing. Moreover, if $\psi^t \geq \psi^{\text{FP}}$, then $\psi^{t+1} \geq \psi^{\text{FP}}$. Indeed, for any $\psi^t \geq \psi^{\text{FP}}$,

$$\psi^{t+1} = \text{mmse}((\sigma^2 + \mu\psi^t)^{-1}) \geq \text{mmse}((\sigma^2 + \mu\psi^{\text{FP}})^{-1}) = \psi^{\text{FP}}.$$

Since $\{\psi^t\}_{t \geq 0}$ is a non-increasing sequence bounded below by ψ^{FP} (noting that $\psi^0 \geq \psi^{\text{FP}}$), we conclude that it converges to ψ^{FP} .

To show that the fixed points of the state evolution correspond to the stationary points of the potential function $\mathcal{F}(\mu, \sigma^2, \psi)$ defined in (19), we compute the derivative:

$$\begin{aligned} \frac{\partial \mathcal{F}(\mu, \sigma^2, \psi)}{\partial \psi} &= \frac{\partial \tau^{-1}}{\partial \psi} \frac{\partial}{\partial \tau^{-1}} I(\mathbf{X}_{\text{sec}}; \mathbf{X}_{\text{sec}} + \sqrt{\tau} \mathbf{Z}) \\ &\quad + \frac{\partial}{\partial \psi} \frac{1}{2\mu} \left[\ln \left(1 + \frac{\mu\psi}{\sigma^2} \right) - \frac{\mu\psi}{\sigma^2 + \mu\psi} \right] \\ &= \frac{-\mu}{(\sigma^2 + \mu\psi)^2} \frac{1}{2} \text{mmse}(1/\tau) + \frac{\mu\psi}{2(\sigma^2 + \mu\psi)^2} \\ &= \frac{\mu}{2(\sigma^2 + \mu\psi)^2} \left[\psi - \text{mmse} \left(\frac{1}{\sigma^2 + \mu\psi} \right) \right], \end{aligned}$$

where the equalities are obtained using $\tau = \sigma^2 + \mu\psi$ and the vector I-MMSE relationship [21, Thm. 2]. Therefore, since $\sigma^2 > 0$ and $\mu > 0$, we have that $\partial \mathcal{F}(\mu, \sigma^2, \psi) / \partial \psi = 0$ corresponds to $\psi = \text{mmse}((\sigma^2 + \mu\psi)^{-1})$, which is the fixed point of the iteration (26).

2) We now prove (25). For $\ell \in [L]$, we denote by $\mathbf{a}_\ell \in \mathbb{R}^B$ the ℓ th section of a vector $\mathbf{a} \in \mathbb{R}^{LB}$. Consider the input to the AMP hard-decision step in iteration $t+1$, which we denote by $\mathbf{s}^t = \mathbf{x}^t + \mathbf{A}^* \mathbf{z}^t \in \mathbb{R}^{LB}$ (see (14), (16)). The MAP estimator $\hat{\mathbf{x}}_\ell^{t+1} = \hat{\mathbf{x}}_\ell^{t+1}(\mathbf{s}_\ell^t)$ in (14) partitions the space \mathbb{R}^B into decision regions. For each \mathbf{x}_ℓ in the support of $p_{\mathbf{X}_{\text{sec}}}$, the decision region is

$$\mathcal{D}(\mathbf{x}_\ell) := \{ \mathbf{s}_\ell^t : \hat{\mathbf{x}}_\ell^{t+1}(\mathbf{s}_\ell^t) = \mathbf{x}_\ell \}. \quad (28)$$

Note that $\mathbb{1}\{\hat{\mathbf{x}}_\ell^{t+1}(\mathbf{s}_\ell^t) = \mathbf{x}_\ell\} = \mathbb{1}\{\mathbf{s}_\ell^t \in \mathcal{D}(\mathbf{x}_\ell)\}$.

The distance between a vector $\mathbf{v} \in \mathbb{R}^B$ and a set $\mathcal{B} \subset \mathbb{R}^B$ is denoted by $d(\mathbf{v}, \mathcal{B}) := \inf\{\|\mathbf{v} - \mathbf{u}\|_2 : \mathbf{u} \in \mathcal{B}\}$. For any $\epsilon > 0$, define the $\psi_{\epsilon,+}, \psi_{\epsilon,-} : \mathbb{R}^B \times \mathbb{R}^B \rightarrow \mathbb{R}$ as follows:

$$\psi_{\epsilon,+}(\mathbf{x}_\ell, \mathbf{s}_\ell^t) = \begin{cases} 1, & \mathbf{s}_\ell^t \in \mathcal{D}(\mathbf{x}_\ell), \\ 0, & d(\mathbf{s}_\ell^t, \mathcal{D}(\mathbf{x}_\ell)) > \epsilon, \\ 1 - d(\mathbf{s}_\ell^t, \mathcal{D}(\mathbf{x}_\ell))/\epsilon, & \text{otherwise,} \end{cases} \quad (29)$$

$$\psi_{\epsilon,-}(\mathbf{x}_\ell, \mathbf{s}_\ell^t) = \begin{cases} 1, & d(\mathbf{s}_\ell^t, \mathcal{D}(\mathbf{x}_\ell)^c) > \epsilon, \\ 0, & \mathbf{s}_\ell^t \in \mathcal{D}(\mathbf{x}_\ell)^c, \\ d(\mathbf{s}_\ell^t, \mathcal{D}(\mathbf{x}_\ell)^c)/\epsilon, & \text{otherwise.} \end{cases} \quad (30)$$

We note that $\psi_{\epsilon,+}, \psi_{\epsilon,-}$ are Lipschitz-continuous (with Lipschitz constant $1/\epsilon$), and

$$\psi_{\epsilon,-}(\mathbf{x}_\ell, \mathbf{s}_\ell^t) \leq \mathbb{1}\{\mathbf{s}_\ell^t \in \mathcal{D}(\mathbf{x}_\ell)\} \leq \psi_{\epsilon,+}(\mathbf{x}_\ell, \mathbf{s}_\ell^t),$$

and thus

$$\begin{aligned} \frac{1}{L} \sum_{\ell=1}^L \psi_{\epsilon,-}(\mathbf{x}_\ell, \mathbf{s}_\ell^t) &\leq \frac{1}{L} \sum_{\ell=1}^L \mathbb{1}\{\hat{\mathbf{x}}_\ell^{t+1}(\mathbf{s}_\ell^t) = \mathbf{x}_\ell\} \\ &\leq \frac{1}{L} \sum_{\ell=1}^L \psi_{\epsilon,+}(\mathbf{x}_\ell, \mathbf{s}_\ell^t). \end{aligned} \quad (31)$$

The results in [22] and [14], [23] imply that for any pseudo-Lipschitz function $\psi : \mathbb{R}^B \times \mathbb{R}^B \rightarrow \mathbb{R}$, the following holds almost surely:

$$\lim_{L \rightarrow \infty} \frac{1}{L} \sum_{\ell=1}^L \psi(\mathbf{x}_\ell, \mathbf{s}_\ell^t) = \mathbb{E}\{\psi(\mathbf{X}_{\text{sec}}, \mathbf{S}_{\tau^t})\}, \quad (32)$$

where $\mathbf{X}_{\text{sec}} \sim p_{\mathbf{X}_{\text{sec}}}$ and \mathbf{S}_{τ^t} is given by (18). This result was proved in [22] for the case $B = 1$, and extended in [14], [23] to the setting of sparse superposition codes where the specific distribution $p_{\mathbf{X}_{\text{sec}}}$ given in Example 2.1 (corresponding to random codebooks) is used. The proof for more general discrete distributions is essentially the same. In (32) and in the equations below, $L/n = \mu$ as $L \rightarrow \infty$.

Applying (32) to the Lipschitz continuous functions $\psi_{\epsilon,+}$ and $\psi_{\epsilon,-}$, we obtain:

$$\begin{aligned} \lim_{L \rightarrow \infty} \frac{1}{L} \sum_{\ell} \psi_{\epsilon,+}(\mathbf{x}_\ell, \mathbf{s}_\ell^t) &= \mathbb{E}\{\psi_{\epsilon,+}(\mathbf{X}_{\text{sec}}, \mathbf{S}_{\tau^t})\}, \quad \text{a.s.} \\ \lim_{L \rightarrow \infty} \frac{1}{L} \sum_{\ell} \psi_{\epsilon,-}(\mathbf{x}_\ell, \mathbf{s}_\ell^t) &= \mathbb{E}\{\psi_{\epsilon,-}(\mathbf{X}_{\text{sec}}, \mathbf{S}_{\tau^t})\} \quad \text{a.s.} \end{aligned} \quad (33)$$

Since $\epsilon > 0$ is arbitrary, from (31) and (33), we almost surely have

$$\begin{aligned} &\lim_{\epsilon \rightarrow 0} \mathbb{E}\{\psi_{\epsilon,-}(\mathbf{X}_{\text{sec}}, \mathbf{S}_{\tau^t})\} \\ &\leq \liminf_{L \rightarrow \infty} \frac{1}{L} \sum_{\ell=1}^L \mathbb{1}\{\hat{\mathbf{x}}_\ell^{t+1}(\mathbf{s}_\ell^t) = \mathbf{x}_\ell\} \\ &\leq \limsup_{L \rightarrow \infty} \frac{1}{L} \sum_{\ell=1}^L \mathbb{1}\{\hat{\mathbf{x}}_\ell^{t+1}(\mathbf{s}_\ell^t) = \mathbf{x}_\ell\} \\ &\leq \lim_{\epsilon \rightarrow 0} \mathbb{E}\{\psi_{\epsilon,+}(\mathbf{X}_{\text{sec}}, \mathbf{S}_{\tau^t})\}. \end{aligned} \quad (34)$$

By the monotone convergence theorem, we have

$$\begin{aligned} \lim_{\epsilon \rightarrow 0} \mathbb{E}\{\psi_{\epsilon,-}(\mathbf{X}_{\text{sec}}, \mathbf{S}_{\tau^t})\} &= \mathbb{P}(\mathbf{S}_{\tau^t} \in \mathcal{D}(\mathbf{X}_{\text{sec}})) = 1 - P_e(\tau^t), \\ \lim_{\epsilon \rightarrow 0} \mathbb{E}\{\psi_{\epsilon,+}(\mathbf{X}_{\text{sec}}, \mathbf{S}_{\tau^t})\} &= \mathbb{P}(\mathbf{S}_{\tau^t} \in \mathcal{D}(\mathbf{X}_{\text{sec}})) = 1 - P_e(\tau^t). \end{aligned} \quad (35)$$

This completes the proof that

$$\lim_{L \rightarrow \infty} \frac{1}{L} \sum_{\ell=1}^L \mathbb{1}\{\hat{\mathbf{x}}_\ell^{t+1}(\mathbf{s}_\ell^t) \neq \mathbf{x}_\ell\} = P_e(\tau^t). \quad (36)$$

Remark 3.1: Consider the setting of Theorem 1 and the MAP decoder for the linear model (3), denoted by $\hat{\mathbf{x}}^{\text{MAP}}$. The (non-rigorous) replica analysis in [24]–[26] shows that the asymptotic user error rate of $\hat{\mathbf{x}}^{\text{MAP}}$ can be analyzed in terms of the error probability for the single-section channel (18). Specifically, when $\mathcal{M}(\mu, \sigma^2)$ in (20) is a singleton,

$$\lim_{L \rightarrow \infty} \frac{1}{L} \sum_{\ell=1}^L \mathbb{1}\{\hat{\mathbf{x}}_\ell^{\text{MAP}} \neq \mathbf{x}_\ell\} = P_e(\tau^*), \quad (37)$$

where the limit is taken with $\frac{L}{n} = \mu$ held constant and

$$\tau^* = \sigma^2 + \mu \mathcal{M}(\mu, \sigma^2). \quad (38)$$

In this setting, and when the sections of the message vector \mathbf{x} are i.i.d. $\sim p_1$ (which corresponds to coding with random codebooks), the MAP decoder is the (joint) ML decoder which was analysed in [1], [2]. Therefore, while [1], [2] provided bounds on the asymptotic achievable region of i.i.d. Gaussian codebooks with ML decoding, equation (37) provides the exact asymptotic achievable region.

Theorem 2 (Spatially coupled Gaussian matrices with AMP decoding): Consider the linear model (3) with a spatially coupled design matrix \mathbf{A} constructed using an (ω, Λ, ρ) base matrix, and the L sections of the message vector \mathbf{x} i.i.d. $\sim p_{\mathbf{X}_{\text{sec}}}$. Let $\hat{\mathbf{x}}^t$ be the AMP hard-decision estimate of \mathbf{x} after iteration t , and recall that $\tau^t \in \mathbb{R}^{\mathcal{C}}$ is an output of the state evolution (8)–(9) and $\mathbf{C} = \Lambda$ in this setting.

1) For any (ω, Λ, ρ) base matrix, each entry of $\tau^t \in \mathbb{R}^{\mathcal{C}}$ is non-increasing in t , and the c th entry converges to a fixed point, denoted by $\tau_c^{\text{SC-FP}}$, for $\mathbf{c} \in [\mathcal{C}]$.

2) For any $\epsilon > 0$, there are constants $\omega_0 < \infty$, $\Lambda_0 < \infty$ and $\rho_0 > 0$ such that, for all $\omega > \omega_0$, $\Lambda > \Lambda_0$ and $0 \leq \rho < \rho_0$, the fixed points $\{\tau_c^{\text{SC-FP}}\}_{\mathbf{c} \in [\mathcal{C}]}$ satisfy

$$\max_{\mathbf{c} \in [\mathcal{C}]} \tau_c^{\text{SC-FP}} \leq \bar{\tau}_\vartheta := \sigma^2 + \vartheta \mu (\max \mathcal{M}(\vartheta \mu, \sigma^2) + \epsilon), \quad (39)$$

where $\vartheta = 1 + (\omega - 1)/\Lambda$, and the set of potential function minimizers $\mathcal{M}(\vartheta \mu, \sigma^2)$ is defined in (20).

3) Fix base matrix parameters $\omega > \omega_0$, $\Lambda > \Lambda_0$, and $0 < \rho < \rho_0$. Fix $\delta > 0$, and let T denote the first iteration for which $\max_{\mathbf{c}} \tau_c^t \leq \tau_c^{\text{SC-FP}} + \delta$. Then the user error rate of the AMP decoder after $T + 1$ iterations satisfies

$$\lim_{L \rightarrow \infty} \frac{1}{L} \sum_{\ell=1}^L \mathbb{1}\{\hat{\mathbf{x}}_\ell^{T+1} \neq \mathbf{x}_\ell\} \stackrel{\text{a.s.}}{=} \frac{1}{\mathcal{C}} \sum_{\mathbf{c}=1}^{\mathcal{C}} P_e(\tau_c^T) \leq P_e(\bar{\tau}_\vartheta + \delta), \quad (40)$$

where the limit is taken with $\frac{L}{n} = \mu$ held constant.

Remark 3.2 (Threshold saturation): Theorem 2 shows that the asymptotic user error rate achievable with a suitable spatially coupled Gaussian matrix and AMP decoding is bounded by $P_e(\bar{\tau}_\vartheta + \delta)$. If $\Lambda \gg \omega$, we have $\vartheta \rightarrow 1$. Therefore, if $\mathcal{M}(\mu, \sigma^2)$ defined in (20) is a singleton, (noting that ϵ in (39) can be arbitrarily small) we have

$$\lim_{\omega \rightarrow \infty} \lim_{\Lambda \rightarrow \infty} \bar{\tau}_\vartheta \rightarrow \tau^*, \quad (41)$$

where τ^* is defined in (38). Therefore, in the limit described in (41), the asymptotic UER of the spatially coupled scheme with AMP decoding is bounded by $P_e(\tau^* + \delta)$ for any fixed $\delta > 0$. This matches the (predicted) asymptotic UER achieved by i.i.d. Gaussian matrices and MAP decoding (Remark 3.1).

This phenomenon, where the performance of message passing decoding in a spatially coupled system matches the MAP (or MMSE) decoding performance in the corresponding uncoupled system, has been shown in other applications and is known as *threshold saturation* [12], [16], [17], [27]–[29].

Proof of Theorem 2: 1) Consider the spatially coupled state evolution (8)–(9) as a single line recursion in the vector $\gamma^t \in \mathbb{R}^{\mathbb{R}}$: for $r \in [\mathbb{R}]$,

$$\gamma_r^{t+1} = \sum_{c=1}^{\mathbb{C}} W_{rc} \text{mmse} \left(\sum_{r'=1}^{\mathbb{R}} W_{r'c} \frac{1}{\sigma^2 + \mu_{\text{inner}} \gamma_{r'}^t} \right). \quad (42)$$

For any base matrix \mathbf{W} with non-negative entries (which includes (ω, Λ, ρ) base matrices), the result in [20, Cor. 4.3] shows that each entry of γ^t is non-increasing in t and converges to a fixed point; we denote these fixed points by $\{\gamma_r^{\text{SC-FP}}\}_{r \in [\mathbb{R}]}$. Since the entries of the state evolution parameter τ^t are non-decreasing in $\{\gamma_r^t\}_{r \in [\mathbb{R}]}$:

$$\tau_c^t = \left[\sum_{r=1}^{\mathbb{R}} \frac{W_{rc}}{\sigma^2 + \mu_{\text{inner}} \gamma_r^t} \right]^{-1}, \quad \text{for } c \in [\mathbb{C}], \quad (43)$$

we conclude that each entry of τ^t is also non-increasing in t and converges to a fixed point; these fixed points are denoted $\{\tau_c^{\text{SC-FP}}\}_{c \in [\mathbb{C}]}$. The arguments used in [20, Cor. 4.3] are similar to those used in the proof of Theorem 1 to show that the uncoupled state evolution parameters converge to fixed points.

2) The result (39) is obtained by using the results in [27] on the fixed points of general coupled recursions. We now describe the steps to apply the results in [27]. The uncoupled state evolution (17) can be written as a single line recursion:

$$\psi^{t+1} = \text{mmse} \left(\frac{1}{\sigma^2 + \mu \psi^t} \right). \quad (44)$$

The uncoupled recursion in (44) and the coupled recursion in (42) correspond exactly to [27, Eqs. (27)–(28)] when μ of the uncoupled system is equal to μ_{inner} of the spatially coupled system and \mathbf{W} is an $(\omega, \Lambda, \rho = 0)$ base matrix. (We will discuss the implications of ρ being a small positive constant later.) Using the same arguments as in [27, Sec. VI.E], and using the vector I-MMSE relationship [21, Thm. 2], we obtain the following result by applying [27, Theorems 1 and 2].

For $\rho = 0$ and any $\epsilon > 0$, there is an $\omega_0 < \infty$ and $\Lambda_0 < \infty$ such that, for all $\omega > \omega_0$ and $\Lambda > \Lambda_0$, the fixed point of (42) satisfies

$$\min \mathcal{M}_1(\mu_{\text{inner}}, \sigma^2) - \epsilon \leq \max_{r \in [\mathbb{R}]} \gamma_r^{\text{SC-FP}} \leq \max \mathcal{M}_1(\mu_{\text{inner}}, \sigma^2) + \epsilon, \quad (45)$$

where

$$\mathcal{M}_1(\mu, \sigma^2) = \left\{ \arg \min_{\psi \in [0, E]} \mathcal{F}_1(\mu, \sigma^2, \psi) \right\}, \quad (46)$$

$$\begin{aligned} \mathcal{F}_1(\mu, \sigma^2, \psi) = & 2 \left(I \left(\mathbf{X}_{\text{sec}}; \sqrt{\frac{1}{\sigma^2 + \mu \psi}} \mathbf{X}_{\text{sec}} + \mathbf{Z} \right) \right. \\ & \left. - I \left(\mathbf{X}_{\text{sec}}; \sqrt{\frac{1}{\sigma^2}} \mathbf{X}_{\text{sec}} + \mathbf{Z} \right) \right. \\ & \left. + \frac{1}{2\mu} \left[\ln \left(1 + \frac{\mu \psi}{\sigma^2} \right) - \frac{\mu \psi}{\sigma^2 + \mu \psi} \right] \right), \quad (47) \end{aligned}$$

and where $\mathbf{X}_{\text{sec}} \sim p_{\mathbf{X}_{\text{sec}}}$ and $\mathbf{Z} \in \mathbb{R}^B$ is a standard Gaussian vector independent of \mathbf{X}_{sec} . Since $\mathcal{F}_1(\mu, \sigma^2, \psi)$ and the potential function $\mathcal{F}(\mu, \sigma^2, \psi)$ defined in (19) are equivalent after removing constant scaling factors and terms that don't depend on ψ , their minimizers with respect to ψ are identical. Therefore, we can write (45) as

$$\min \mathcal{M}(\mu_{\text{inner}}, \sigma^2) - \epsilon \leq \max_{r \in [\mathbb{R}]} \gamma_r^{\text{SC-FP}} \leq \max \mathcal{M}(\mu_{\text{inner}}, \sigma^2) + \epsilon, \quad (48)$$

where $\mathcal{M}(\mu, \sigma^2)$ is the set of minimizers of $\mathcal{F}(\mu, \sigma^2, \psi)$.

Now we consider the effect of ρ being a small positive constant on the fixed point of the state evolution. We study this scenario as ρ needs to be lower bounded by a strictly positive constant for the AMP concentration result in (40) to hold. First, the $\text{mmse}(\text{snr})$ function defined in (10) is a smooth function of snr on $(0, \infty)$ [19, Prop. 7]. Therefore, the right-hand-side of (42) is a smooth function of the entries of \mathbf{W} . Hence, the fixed point of the state evolution recursion (42) is a smooth function of ρ . For $\rho \geq 0$, denoting this fixed point by $\{\gamma_r^{\text{SC-FP}}(\rho)\}_{r \in [\mathbb{R}]}$, and letting

$$\Delta(\rho) := \max_{r \in [\mathbb{R}]} \left| \gamma_r^{\text{SC-FP}}(\rho) - \gamma_r^{\text{SC-FP}}(0) \right|,$$

we have $\Delta(\rho) \rightarrow 0$ as $\rho \rightarrow 0$. Consequently, the result for $(\omega, \Lambda, \rho = 0)$ base matrices in (48) holds for $(\omega, \Lambda, \rho > 0)$ base matrices with the deviation ϵ replaced by the slightly larger value $\epsilon + \Delta(\rho)$. Equivalently, since $\epsilon > 0$ is arbitrary and $\Delta(\rho)$ is a smooth function with $\Delta(0) = 0$, there exists a $\rho_0 > 0$ such that, for all $\rho < \rho_0$, the result (48) holds for $(\omega, \Lambda, \rho > 0)$ base matrices.

We now obtain (39) using (48). For $c \in [\mathbb{C}]$, we have

$$\begin{aligned} \tau_c^{\text{SC-FP}} &= \left[\sum_{r=1}^{\mathbb{R}} \frac{W_{rc}}{\sigma^2 + \mu_{\text{inner}} \gamma_r^{\text{SC-FP}}} \right]^{-1} \\ &\leq \left[\frac{\sum_{r=1}^{\mathbb{R}} W_{rc}}{\sigma^2 + \mu_{\text{inner}} \max_{r' \in [\mathbb{R}]} \gamma_{r'}^{\text{SC-FP}}} \right]^{-1} \\ &\leq \sigma^2 + \mu_{\text{inner}} (\max \mathcal{M}(\mu_{\text{inner}}, \sigma^2) + \epsilon), \end{aligned}$$

where the last inequality is obtained using the $\sum_{r=1}^{\mathbb{R}} W_{rc} = 1$ constraint on base matrices, and the upper bound in (48). The result (39) follows by recalling from (6) that $\mu_{\text{inner}} = \vartheta \mu$, where $\vartheta = 1 + (\omega - 1)/\Lambda$.

3) We now prove (40). Consider the input to the AMP hard-decision step in iteration $t + 1$, which we denote by $s^t =$

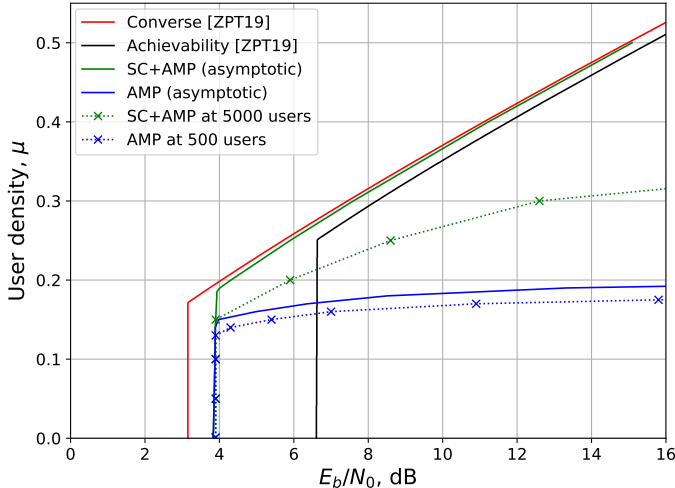


Fig. 2. Achievability regions for massive multiple access at a user payload of 8 bits ($B = 2^8$), when the maximum tolerated UER is 10^{-3} .

TABLE I
OPTIMIZED VALUES OF COUPLING WIDTH ω USED IN FIG. 2.

| μ | 0.15 | 0.20 | 0.25 | 0.30 | 0.33 |
|----------|------|------|------|------|------|
| ω | 5 | 5 | 6 | 11 | 14 |

$\mathbf{x}^t + (\tilde{\mathbf{S}}^t \odot \mathbf{A})^* \mathbf{z}^t$ (see (7), (14)). For $\ell \in [L]$, we denote by $\mathbf{a}_\ell \in \mathbb{R}^B$ the ℓ th section of a vector $\mathbf{a} \in \mathbb{R}^{LB}$.

The results in [30] and [14] imply that for any pseudo-Lipschitz function $\psi : \mathbb{R}^B \times \mathbb{R}^B \rightarrow \mathbb{R}$, the following holds almost surely:

$$\lim_{L \rightarrow \infty} \frac{1}{L} \sum_{\ell=1}^L \psi(\mathbf{x}_\ell, \mathbf{s}_\ell^t) = \frac{1}{C} \sum_{c=1}^C \mathbb{E}\{\psi(\mathbf{X}_{\text{sec}}, \mathbf{S}_{\tau_c^t})\}, \quad (49)$$

where the limit is taken with $L/n = \mu$ held constant, $\mathbf{X}_{\text{sec}} \sim p_{\mathbf{X}_{\text{sec}}}$ and $\mathbf{S}_{\tau_c^t}$ is given by (18). This result was proved in [30] for $B = 1$, and extended in [14] to the setting of sparse superposition codes where the specific distribution $p_{\mathbf{X}_{\text{sec}}}$ given in Example 2.1 (corresponding to random codebooks) is used. The proof for more general discrete distributions is essentially the same.

Then, following the same steps as (28)–(35) (using (49) instead of (32) in (33)) gives the desired result. ■

A. Numerical Results

In Fig. 2, we plot the achievable regions of AMP decoding with i.i.d. and spatially coupled Gaussian codebooks, i.e., when the design matrix \mathbf{A} is i.i.d. or spatially coupled Gaussian, and the sections of \mathbf{x} are drawn i.i.d. from p_1 . Specifically, for a list of user densities μ , we plot the minimum $\frac{E_b}{N_0}$ required by the coding schemes to achieve a UER of less than 10^{-3} , when the user payload is $\log_2 B = 8$ bits.

The asymptotic achievable region with AMP decoding of i.i.d. Gaussian codebooks is given by Theorem 1 (solid blue line), and that of spatially coupled Gaussian codebooks given by Theorem 2 and Remark 3.2 (solid green line). We observe that the achievable region of spatially coupled Gaussian codebooks with efficient AMP decoding is strictly larger the

achievability bound in [2] (black line), which is based on i.i.d. Gaussian codebooks and ML decoding. It also nearly matches the converse bound (red line) for $\mu \geq 0.2$. Also observe that for $\mu \leq 0.15$, the minimum $\frac{E_b}{N_0}$ required by the i.i.d. and spatially coupled coding schemes with AMP decoding is the same. However, the gap between the two achievable regions increases sharply for larger μ . Furthermore, the shape of the solid blue curve suggests that it might be impossible to achieve $\text{UER} \leq 10^{-3}$ with i.i.d. Gaussian codebooks and AMP decoding above a certain user density ($\mu \approx 0.2$).

We also show the simulated performance of i.i.d. and spatially coupled coding schemes with 500 and 5000 users, respectively (dotted lines with crosses). For a list of user densities μ , the crosses show the minimum $\frac{E_b}{N_0}$ at which the coding scheme achieves an average UER less than 10^{-3} (averaged over many independent trials). Discrete Cosine Transform (DCT) based design matrices were used to reduce decoding complexity and memory usage. The error rates obtained using DCT and Gaussian matrices are similar for large matrix sizes. The simulations for the spatially coupled coding scheme used $(\omega, \Lambda = 50, \rho = 0)$ base matrices. The coupling width ω was optimized for each user density μ (see Table I).

We observe that for both i.i.d. and spatially coupled coding schemes, the finite user and asymptotic curves match at low user densities. For the i.i.d. coding scheme, although a gap between the two curves appears above $\mu = 0.13$, their overall shape remains similar. For the spatially coupled scheme, the gap between the two curves appears above $\mu = 0.15$, and increases with μ . This gap is a finite length effect, due to the relatively small values of base matrix parameters.

Table I shows the values of the optimized coupling widths used in Fig. 2, for user densities above the threshold ($\mu = 0.15$) at which the spatially coupled coding scheme has an advantage over the i.i.d. coding scheme. At user densities lower than this threshold, a range of coupling widths (including the uncoupled case $\omega = 1$) achieve similar UERs. We see that the optimal coupling width increases with the user density.

IV. LARGE USER PAYLOADS

When coding with random codebooks, i.e., when the sections of \mathbf{x} are drawn i.i.d. from p_1 , the size B of each of the sections in \mathbf{x} increases exponentially with the user payload ($\log_2 B$ bits). For very large B it is infeasible to evaluate the potential function (19). The potential function is needed to compute the asymptotic UER bounds in Theorems 1 and 2 (see (25) and (40)). In this section we bound the asymptotic UER achieved by i.i.d. and spatially coupled Gaussian codebooks with AMP decoding, when the user payload is large. Both results (Theorems 3 and 4) utilize the following Lemma.

Lemma 4.1 (Asymptotic UER bound): Consider the setting of either Theorem 1 or 2, and take the distribution $p_{\mathbf{X}_{\text{sec}}}$ to be p_1 . Let $\hat{\mathbf{x}}^t$ be the AMP hard-decision estimate of \mathbf{x} after iteration t , and recall that $\psi^t \in \mathbb{R}^C$ is an output of the state

evolution (8)–(9). Then we have that the following limit exists almost surely and satisfies:

$$\frac{1}{2\mathbf{C}} \sum_{\mathbf{c}=1}^{\mathbf{C}} \frac{\psi_{\mathbf{c}}^t}{E} \leq \lim_{L \rightarrow \infty} \frac{1}{L} \sum_{\ell=1}^L \mathbb{1}\{\hat{\mathbf{x}}_{\ell}^t \neq \mathbf{x}_{\ell}\} \leq \frac{4}{\mathbf{C}} \sum_{\mathbf{c}=1}^{\mathbf{C}} \frac{\psi_{\mathbf{c}}^t}{E}, \quad (50)$$

where the limit is taken with $\frac{L}{n} = \mu$ held constant. Recall that $\mathbf{C} = 1$ when the design matrix \mathbf{A} is has i.i.d. Gaussian entries $\mathcal{N}(0, \frac{1}{n})$.

Proof: The existence of the limit in (50) is shown in Theorems 1 and 2. For $\ell \in [L]$, we denote by $\mathbf{a}_{\ell} \in \mathbb{R}^B$ the ℓ th section of a vector $\mathbf{a} \in \mathbb{R}^{LB}$. Let \mathbf{x}^{t+1} be the AMP estimate of \mathbf{x} after iteration $t+1$ (defined in (13)).

It was proved in [14] that the MSE of the AMP decoder after iteration $t \geq 0$ converges almost surely to the following limit:

$$\begin{aligned} \lim_{L \rightarrow \infty} \frac{\|\mathbf{x}^{t+1} - \mathbf{x}\|^2}{L} &= \frac{1}{\mathbf{C}} \sum_{\mathbf{c}=1}^{\mathbf{C}} \psi_{\mathbf{c}}^{t+1} \\ &= \frac{1}{\mathbf{C}} \sum_{\mathbf{c}=1}^{\mathbf{C}} \mathbb{E}\left\{\|\mathbf{X}_{\text{sec}} - \mathbb{E}[\mathbf{X}_{\text{sec}} | \mathbf{X}_{\text{sec}} + \sqrt{\tau_{\mathbf{c}}^t} \mathbf{Z}]\|^2\right\}, \end{aligned} \quad (51)$$

where $\mathbf{X}_{\text{sec}} \sim p_{\mathbf{X}_{\text{sec}}}$ and \mathbf{Z} is a standard Gaussian vector independent of \mathbf{X}_{sec} . The last equality in (51) follows from the definition of $\psi_{\mathbf{c}}^t$ (see (9) and (10)). Moreover, using the result (40) (noting that the first equality in (40) holds for $t \geq 0$), we have

$$\begin{aligned} \lim_{L \rightarrow \infty} \frac{1}{L} \sum_{\ell=1}^L \mathbb{1}\{\hat{\mathbf{x}}_{\ell}^{t+1} \neq \mathbf{x}_{\ell}\} &= \frac{1}{\mathbf{C}} \sum_{\mathbf{c}=1}^{\mathbf{C}} P_e(\tau_{\mathbf{c}}^t) \\ &= \frac{1}{\mathbf{C}} \sum_{\mathbf{c}=1}^{\mathbf{C}} \mathbb{E}\left[\mathbb{1}\{\mathbf{X}_{\text{sec}} \neq \hat{\mathbf{X}}(\mathbf{X}_{\text{sec}} + \sqrt{\tau_{\mathbf{c}}^t} \mathbf{Z})\}\right] \\ &= \frac{1}{2E} \frac{1}{\mathbf{C}} \sum_{\mathbf{c}=1}^{\mathbf{C}} \mathbb{E}\left[\|\mathbf{X}_{\text{sec}} - \hat{\mathbf{X}}(\mathbf{X}_{\text{sec}} + \sqrt{\tau_{\mathbf{c}}^t} \mathbf{Z})\|^2\right]. \end{aligned} \quad (52)$$

Here $\hat{\mathbf{X}}(\cdot)$ is the MAP estimator of \mathbf{X}_{sec} , i.e.,

$$\hat{\mathbf{X}}(\mathbf{s}) = \arg \max_{\mathbf{x}'} \mathbb{P}(\mathbf{X}_{\text{sec}} = \mathbf{x}' | \mathbf{X}_{\text{sec}} + \sqrt{\tau_{\mathbf{c}}^t} \mathbf{Z} = \mathbf{s}).$$

The second equality in (52) follows from (21), noting that $P_e(\tau_{\mathbf{c}}^t) = \mathbb{P}(\mathbf{X}_{\text{sec}} \neq \hat{\mathbf{X}}(\mathbf{X}_{\text{sec}} + \sqrt{\tau_{\mathbf{c}}^t} \mathbf{Z}))$. The third equality is obtained by noticing that for $\mathbf{X}_{\text{sec}} \sim p_1$, the squared error of the MAP estimator $\hat{\mathbf{X}}(\mathbf{s})$ (defined in (15)) satisfies

$$\|\hat{\mathbf{X}}(\mathbf{s}) - \mathbf{X}_{\text{sec}}\|^2 = 2E \mathbb{1}\{\hat{\mathbf{X}}(\mathbf{s}) \neq \mathbf{X}_{\text{sec}}\}. \quad (53)$$

Among estimators of \mathbf{X}_{sec} from $\mathbf{S} = \mathbf{X}_{\text{sec}} + \sqrt{\tau_{\mathbf{c}}^t} \mathbf{Z}$, the expected squared loss is minimized by the conditional expectation. Therefore, for $\mathbf{c} \in [\mathbf{C}]$,

$$\begin{aligned} \mathbb{E}\left\{\|\mathbf{X}_{\text{sec}} - \mathbb{E}[\mathbf{X}_{\text{sec}} | \mathbf{X}_{\text{sec}} + \sqrt{\tau_{\mathbf{c}}^t} \mathbf{Z}]\|^2\right\} \\ \leq \mathbb{E}\left\{\|\mathbf{X}_{\text{sec}} - \hat{\mathbf{X}}(\mathbf{X}_{\text{sec}} + \sqrt{\tau_{\mathbf{c}}^t} \mathbf{Z})\|^2\right\}. \end{aligned} \quad (54)$$

Using (54) to compare the limits in (51) and (52), we obtain first inequality in (50).

To prove the second inequality in (50), we first notice that for the prior p_1 , the hard-decision estimator $\hat{\mathbf{x}}_{\ell}^{t+1}$ defined in (15) can equivalently be written as follows. For $j \in \text{sec}(\ell)$:

$$\hat{\mathbf{x}}_j^{t+1} = \begin{cases} \sqrt{E} & \text{if } x_j^{t+1} > x_i^{t+1} \text{ for all } i \in \text{sec}(\ell) \setminus j, \\ 0 & \text{otherwise.} \end{cases} \quad (55)$$

Here \mathbf{x}^{t+1} is the AMP estimate computed according to (7) and (13).

Let $j^* \in \text{sec}(\ell)$ denote the index of the unique non-zero entry of \mathbf{x} in section $\ell \in [L]$, i.e., $x_{j^*} = \sqrt{E}$. From (13), we note that the sum of the entries in each section of \mathbf{x}^{t+1} equals \sqrt{E} . The decision rule (55) then implies that $\hat{\mathbf{x}}_{j^*}^{t+1}$ is less than or equal to $\sqrt{E}/2$ whenever $\hat{\mathbf{x}}_{\ell}^{t+1} \neq \mathbf{x}_{\ell}$. Therefore,

$$\hat{\mathbf{x}}_{\ell}^{t+1} \neq \mathbf{x}_{\ell} \quad \text{implies} \quad \|\mathbf{x}_{\ell}^{t+1} - \mathbf{x}_{\ell}\|^2 \geq E/4. \quad (56)$$

Therefore,

$$\frac{1}{L} \sum_{\ell=1}^L \mathbb{1}\{\hat{\mathbf{x}}_{\ell}^{t+1} \neq \mathbf{x}_{\ell}\} \leq \frac{1}{L} \sum_{\ell=1}^L \frac{4\|\mathbf{x}_{\ell}^{t+1} - \mathbf{x}_{\ell}\|^2}{E}. \quad (57)$$

Combining (57) with (51) yields the second inequality in (50). \blacksquare

Theorem 3 (AMP decoding of i.i.d. Gaussian codebooks at large user payloads): Consider the setting of Theorem 1 and take the distribution $p_{\mathbf{X}_{\text{sec}}}$ to be p_1 . The user error rate of the AMP decoder after its first iteration exhibits the following phase transition for sufficiently large payloads $\log_2 B$.

1) For any $\delta \in (0, \frac{1}{2})$, let $f_{B,\delta} := \frac{B^{-k\delta^2}}{\delta\sqrt{\ln B}}$ where k is a positive constant. If

$$\mu \log_2 B < \frac{1}{2} \left(\frac{1}{(1+\delta)\ln 2} - \frac{1}{E_b/N_0} \right), \quad (58)$$

then $\lim_{L \rightarrow \infty} \frac{1}{L} \sum_{\ell=1}^L \mathbb{1}\{\hat{\mathbf{x}}_{\ell}^1 \neq \mathbf{x}_{\ell}\} \leq f_{B,\delta}$.

2) For any $\delta \in (0, 1)$, let $g_{B,\delta} := B^{-k_1\delta^2}$ where k_1 is a positive constant. If

$$\mu \log_2 B > \frac{1}{2(1-g_{B,\delta})} \left(\frac{1}{(1-\frac{\delta}{2})\ln 2} - \frac{1}{E_b/N_0} \right), \quad (59)$$

then $\lim_{L \rightarrow \infty} \frac{1}{L} \sum_{\ell=1}^L \mathbb{1}\{\hat{\mathbf{x}}_{\ell}^t \neq \mathbf{x}_{\ell}\} \geq (1-g_{B,\delta})/2$ for all $t \geq 1$. In both statements, the limits exist and are taken with $\frac{L}{n} = \mu$ held constant.

Proof: From Lemma 4.1, we know that the asymptotic UER after each iteration $t \geq 1$ satisfies

$$\frac{\psi^t}{2E} \leq \lim_{L \rightarrow \infty} \frac{1}{L} \sum_{\ell=1}^L \mathbb{1}\{\hat{\mathbf{x}}_{\ell}^t \neq \mathbf{x}_{\ell}\} \leq \frac{4\psi^t}{E}, \quad (60)$$

where ψ^t is the output of the state evolution (17) after the t th iteration.

Using state evolution variables τ^t and ψ^t defined in (17), let

$$\nu^t := \frac{E}{\tau^t \ln B} = \frac{E}{(\sigma^2 + \mu\psi^t) \ln B}. \quad (61)$$

From [14, Lem. 4.1] we know that for sufficiently large B and any $\delta \in (0, \frac{1}{2})$, $\tilde{\delta} \in (0, 1)$, we have

$$(1 - g_{B, \tilde{\delta}}) \mathbb{1}\{\nu^t < 2 - \tilde{\delta}\} < \frac{\psi^{t+1}}{E} \leq 1 - (1 - f_{B, \delta}) \mathbb{1}\{\nu^t > 2 + \delta\}, \quad (62)$$

where $g_{B, \tilde{\delta}}$, $f_{B, \delta}$ are defined in the theorem statement. Using (61) in (62) and recalling that $E = E_b \log_2 B$, $\sigma^2 = \frac{N_0}{2}$, we obtain

$$\frac{\psi^{t+1}}{E} \begin{cases} \leq f_{B, \delta} & \text{if } \frac{\psi^t}{E} < \frac{\frac{2}{2+\delta} - \frac{\ln 2}{E_b/N_0}}{2\mu \ln B}, \\ > (1 - g_{B, \tilde{\delta}}) & \text{if } \frac{\psi^t}{E} > \frac{\frac{2}{2-\delta} - \frac{\ln 2}{E_b/N_0}}{2\mu \ln B}. \end{cases} \quad (63)$$

We obtain the first part of the theorem by substituting the initial condition $\psi^0 = E$ into the first condition in (63), and using a different positive constant in the definition of $f_{B, \delta}$ to account for the factor of 4 in the upper bound in (60).

We prove the second statement of the theorem by showing that under (59), $\frac{\psi^t}{E} > (1 - g_{B, \tilde{\delta}})$ for all $t \geq 1$. Combining this with the lower bound in (60) then yields the required result.

Noting that $\psi^0/E = 1$, assume towards induction that $\frac{\psi^t}{E} > (1 - g_{B, \tilde{\delta}})$ for some $t \geq 0$. Then, from (61) we have

$$\begin{aligned} \nu^t &< \frac{1}{(\sigma^2/E + \mu(1 - g_{B, \tilde{\delta}})) \ln B} \\ &= \frac{1}{\ln 2 / (2E_b/N_0) + \mu \log_2 B (1 - g_{B, \tilde{\delta}}) \ln 2}. \end{aligned} \quad (64)$$

Therefore a sufficient condition for $\nu^t < (2 - \tilde{\delta})$ is

$$\left(\frac{N_0}{2E_b} + \mu \log_2 B (1 - g_{B, \tilde{\delta}}) \right) \ln 2 > \frac{1}{2 - \tilde{\delta}}. \quad (65)$$

Rearranging, we obtain the condition in (59). From (62) we see that under this condition, $\psi^{t+1}/E > (1 - g_{B, \tilde{\delta}})$. This completes the proof of the induction step, and hence the theorem. \blacksquare

Remark 4.1: From (58) and (59), we see that for any fixed values of μ and $\frac{E_b}{N_0}$, the UER of AMP decoding is lower bounded by a value that approaches 1/2 with growing B . Therefore, the interesting regime for large user payloads is when the spectral efficiency

$$S := \mu \log_2 B = \frac{L \log_2 B}{n} \text{ bits/transmission}, \quad (66)$$

is of constant order. (The spectral efficiency is the total number of bits sent by all the users per channel use.) Theorem 3 can be extended to this asymptotic regime where $L, n, \log_2 B$ all tend to infinity with the spectral efficiency held constant. In this case, the user error rate of the AMP decoder exhibits the following phase transition in this large system limit.

$$\lim_{L, B, n \rightarrow \infty} \frac{1}{L} \sum_{\ell=1}^L \mathbb{1}\{\hat{\mathbf{x}}_\ell^1 \neq \mathbf{x}_\ell\} \begin{cases} = 0 & \text{if } S < S_{\text{BP}}, \\ \geq \frac{1}{2} & \text{otherwise,} \end{cases} \quad (67)$$

where S_{BP} is the belief propagation (BP) threshold

$$S_{\text{BP}} := \frac{1}{2} \left(\frac{1}{\ln 2} - \frac{1}{E_b/N_0} \right). \quad (68)$$

From (67), we see that positive spectral efficiencies are achievable in this large system setting using i.i.d. Gaussian codebooks and AMP decoding if and only if $\frac{E_b}{N_0} > \ln 2$.

From Remark 4.1, we see that for large user payloads and spectral efficiencies less than the BP threshold S_{BP} , one does not require spatial coupling for reliable AMP decoding. The following result shows that any spectral efficiency above S_{BP} and below the converse can be achieved using spatially coupled Gaussian codebooks and AMP decoding.

Theorem 4 (AMP decoding of spatially coupled Gaussian codebooks at large user payloads): Consider the setting of Theorem 2 and take the distribution $p_{\mathbf{X}_{\text{sec}}}$ to be p_1 . Let $\vartheta = 1 + \frac{\omega-1}{\Lambda}$, $\mu = \frac{L}{n}$, $\text{SNR} = \frac{2E_b}{N_0} \mu \log_2 B$, and define

$$\Delta := \frac{1}{2\vartheta} \ln(1 + \vartheta \text{SNR}) - \mu \ln B, \quad (69)$$

$$\omega^* := \left(\frac{\vartheta \text{SNR}^2}{1 + \vartheta \text{SNR}} \right) \frac{1}{\Delta}, \quad (70)$$

$$\rho^* := \min \left\{ \frac{\Delta}{3 \text{SNR}}, \frac{1}{2} \right\}. \quad (71)$$

Let δ be an arbitrary constant in $(0, \min\{\frac{\Delta}{2\mu \ln B}, \frac{1}{2}\})$ and S_{opt} be the solution to

$$S_{\text{opt}} = \frac{1}{2} \log_2 \left(1 + S_{\text{opt}} \frac{2E_b}{N_0} \right). \quad (72)$$

1) If the spectral efficiency satisfies

$$\frac{1}{\vartheta} S_{\text{BP}} \leq \mu \log_2 B < \frac{1}{\vartheta} S_{\text{opt}}, \quad (73)$$

and the base matrix parameters satisfy $\omega > \omega^*$ and $0 < \rho \leq \rho^*$, then, for $t \geq 1$ and $\mathbf{c} \leq \max\{\frac{\omega t}{\omega^*}, \lceil \frac{\Delta}{2} \rceil\}$, we have

$$\psi_{\mathbf{c}}^t = \psi_{\Lambda - \mathbf{c} + 1}^t \leq E h_{B, \delta} \quad (74)$$

for sufficiently large B , where $E = E_b \log_2 B$, $h_{B, \delta} := \frac{B^{-k_2 \delta^2}}{\delta \sqrt{\ln B}}$ and k_2 is a positive constant.

2) Let T denote the first iteration for which $\max_{\mathbf{c}} \psi_{\mathbf{c}}^t \leq E h_{B, \delta}$. Then we have

$$T \leq \left\lceil \frac{\Lambda \omega^*}{2\omega} \right\rceil, \quad (75)$$

and the user error rate of the AMP decoder after T iterations satisfies

$$\lim_{L \rightarrow \infty} \frac{1}{L} \sum_{\ell=1}^L \mathbb{1}\{\hat{\mathbf{x}}_\ell^T \neq \mathbf{x}_\ell\} \leq 4 h_{B, \delta}, \quad (76)$$

where the limit is taken with $\frac{L}{n} = \mu$ held constant.

Proof: The first part of Theorem 4 is a direct application of the state evolution analysis of spatially coupled sparse superposition codes for channel coding over the (single user) AWGN channel [14, Prop. 4.1]. The main change of variables required is that the signal-to-noise ratio in the AWGN channel is replaced by $\text{SNR} = \frac{L(E/n)}{\sigma^2} = \frac{2E_b}{N_0} \mu \log_2 B$. Another change is that the AWGN rate $R = \frac{L \ln B}{n}$ in [14] is replaced by $\mu \ln B$. We note that a positive solution to (72) exists if and only if $\frac{E_b}{N_0} > \ln 2$. The second part of Theorem is a direct application of the upper bound given in Lemma 4.1. \blacksquare

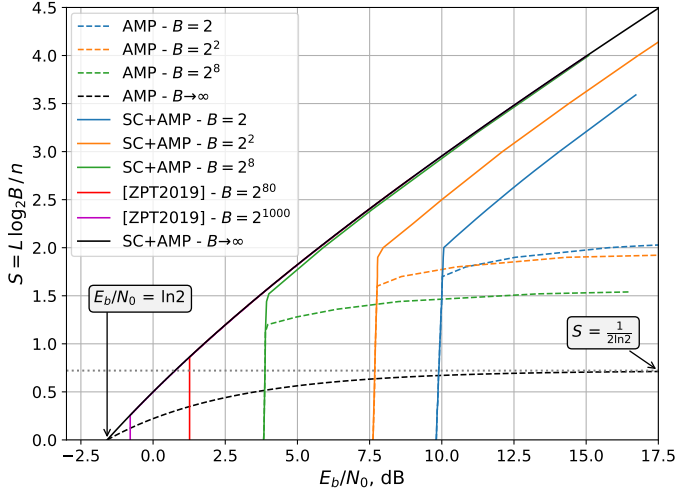


Fig. 3. Achievable regions for massive multiple access at different user payloads ($\log_2 B$ bits) using either i.i.d. or spatially coupled Gaussian codebooks with AMP decoding. The results at finite B show the minimum E_b/N_0 required to achieve $\text{UER} \leq 10^{-3}$.

Remark 4.2 (Parameter choice): Consider spectral efficiency $S = \mu \log_2 B$ bits/transmission. For any spectral efficiency $S < S_{\text{opt}}$, or equivalently any $\frac{E_b}{N_0} > \frac{2^{2S}-1}{2S}$ (which matches the converse bound in [2] with $B \rightarrow \infty$ and the target PUPE $\epsilon \rightarrow 0$), we can choose design parameters as follows to guarantee that the AMP decoder achieves a small UER at large payloads.

1) If $S < S_{\text{BP}}$, or equivalently $\frac{E_b}{N_0} > (\frac{1}{\ln 2} - 2S)^{-1}$ for $S < \frac{1}{2 \ln 2}$, then using i.i.d. Gaussian codebooks guarantees that the UER is bounded by a small constant at large payloads (Theorem 3).

2) If $S_{\text{BP}} \leq S < S_{\text{opt}}$, we can choose the base matrix parameters ω and Λ as follows to satisfy the conditions of Theorem 4. Let $\vartheta_0 = S_{\text{opt}}/S$, first choose $\omega > \omega^*(\vartheta_0)$ (with ϑ in (70) replaced by ϑ_0). Then choose Λ large enough that $\vartheta = 1 + \frac{\omega-1}{\Lambda} \leq \vartheta_0$. This ensures that $S < S_{\text{opt}}/\vartheta$ and $\omega > \omega^*(\vartheta)$.

Remark 4.3: Theorem 4 can be extended to the setting where $L, n, \log_2 B$ all tend to infinity with the spectral efficiency $S = L \log_2 B/n$ held constant (see Remark 4.1). In this asymptotic regime, the result states that for any $S_{\text{BP}} \leq S < S_{\text{opt}}$, the UER with AMP decoding converges almost surely to 0.

A. Numerical Results

Fig. 3 shows the achievable regions of i.i.d. and spatially coupled Gaussian codebooks with AMP decoding, in the large system limit of $L, n, \log_2 B$ all tending to infinity with the spectral efficiency $S = L \log_2 B/n$ held constant (Remarks 4.1 and 4.3). The dashed black line is the achievable region for i.i.d. Gaussian codebooks and the solid black line for spatially coupled codebooks. From (68), we note that i.i.d. Gaussian codebooks with AMP decoding cannot achieve spectral efficiencies $S \geq \frac{1}{2 \ln 2} \approx 0.7213$ (asymptote of the dashed black line). We note that the solid black line matches the converse bound in [2] with $B \rightarrow \infty$ and the target PUPE $\epsilon \rightarrow 0$.

The solid and dashed black lines split Fig. 3 into three distinct regions, which are sometimes referred to as the ‘easy’,

‘hard’, and ‘impossible’ regions of inference in statistical physics [31]:

- 1) Below dashed black line: achievable with i.i.d. Gaussian codebooks and AMP decoding.
- 2) Between solid and dashed black lines: achievable with spatially coupled Gaussian codebooks and AMP decoding, or the MAP decoder with i.i.d. Gaussian codebooks.
- 3) Above solid black line: not achievable by any scheme.

In Fig. 3, we also plot the achievable regions of i.i.d. Gaussian codebooks (dashed) and spatially coupled codebooks (solid) with AMP decoding at several finite payloads $\log_2 B$ (with $L, n \rightarrow \infty$ and the user density μ held constant). For $B = 2, 2^2, 2^8$, we use the same setup as Fig. 2, and find the smallest $\frac{E_b}{N_0}$ such that the coding scheme achieves $\text{UER} \leq 10^{-3}$. For $B = 2^{80}, 2^{1000}$, it is computationally infeasible to evaluate the potential function (19), so we plot the achievability bound from [2] (red and purple curves).

For spatially coupled Gaussian codebooks with AMP decoding, the achievable region gets larger as the user payload increases, but at high spectral efficiencies (e.g. $S > 1.5$), the improvement is insignificant after roughly $\log_2 B = 8$ bits. Therefore, it is possible to communicate reliably at high spectral efficiencies with near-minimal $\frac{E_b}{N_0}$ even when the user payload is finite. For i.i.d. Gaussian codebooks with AMP decoding, there is a tradeoff in the achievable region as the user payload increases: a lower E_b/N_0 is required to communicate reliably at low spectral efficiencies, but the maximum achievable spectral efficiency decreases.

REFERENCES

- [1] Y. Polyanskiy, “A perspective on massive random-access,” in *Proc. IEEE Int. Symp. Inf. Theory*, 2017, pp. 2523–2527.
- [2] I. Zadik, Y. Polyanskiy, and C. Thrampoulidis, “Improved bounds on Gaussian MAC and sparse regression via Gaussian inequalities,” in *Proc. IEEE Int. Symp. Inf. Theory*, 2019, pp. 430–434.
- [3] S. S. Kowshik, K. Andreev, A. Frolov, and Y. Polyanskiy, “Energy efficient random access for the quasi-static fading MAC,” in *Proc. IEEE Int. Symp. Inf. Theory*, 2019, pp. 2768–2772.
- [4] S. S. Kowshik and Y. Polyanskiy, “Fundamental limits of many-user MAC with finite payloads and fading,” *arXiv:1901.06732*, 2020, <https://arxiv.org/abs/1901.06732>.
- [5] X. Chen, T. Chen, and D. Guo, “Capacity of Gaussian many-access channels,” *IEEE Trans. Inf. Theory*, vol. 63, no. 6, pp. 3516–3539, June 2017.
- [6] J. Ravi and T. Koch, “Capacity per unit-energy of Gaussian many-access channels,” in *Proc. IEEE Int. Symp. Inf. Theory*, 2019.
- [7] —, “On the per-user probability of error in Gaussian many-access channels,” in *Proceedings International Zurich Seminar on Information and Communication (IZS)*, 2020, pp. 139 – 143.
- [8] —, “Capacity per unit-energy of Gaussian random many-access channels,” *arXiv:2005.07436*, 2020, <https://arxiv.org/abs/2005.07436>.
- [9] V. K. Amalladinne, A. K. Pradhan, C. Rush, J.-F. Chamberland, and K. R. Narayanan, “On approximate message passing for unsourced access with coded compressed sensing,” *arXiv:2001.03705*, 2020, <https://arxiv.org/abs/2001.03705>.
- [10] A. Fengler, P. Jung, and G. Caire, “Unsourced multiuser sparse regression codes achieve the symmetric MAC capacity,” *arXiv:2001.04217*, 2020, <https://arxiv.org/abs/2001.04217>.
- [11] F. Krzakala, M. Mézard, F. Sausset, Y. F. Sun, and L. Zdeborová, “Statistical-physics-based reconstruction in compressed sensing,” *Phys. Rev. X*, vol. 2, p. 021005, May 2012.

- [12] D. L. Donoho, A. Javanmard, and A. Montanari, "Information-theoretically optimal compressed sensing via spatial coupling and approximate message passing," *IEEE Trans. Inf. Theory*, vol. 59, no. 11, pp. 7434–7464, Nov. 2013.
- [13] J. Barbier and F. Krzakala, "Approximate message-passing decoder and capacity achieving sparse superposition codes," *IEEE Trans. Inf. Theory*, vol. 63, no. 8, pp. 4894–4927, Aug. 2017.
- [14] C. Rush, K. Hsieh, and R. Venkataramanan, "Capacity-achieving spatially coupled sparse superposition codes with AMP decoding," *arXiv:2002.07844*, 2020, <https://arxiv.org/abs/2002.07844>.
- [15] K. Hsieh, C. Rush, and R. Venkataramanan, "Spatially coupled sparse regression codes: Design and state evolution analysis," in *Proc. IEEE Int. Symp. Inf. Theory*, June 2018, pp. 1016–1020.
- [16] S. Kudekar, T. J. Richardson, and R. L. Urbanke, "Threshold saturation via spatial coupling: Why convolutional LDPC ensembles perform so well over the BEC," *IEEE Trans. Inf. Theory*, vol. 57, no. 2, pp. 803–834, Feb 2011.
- [17] S. Kudekar, T. Richardson, and R. L. Urbanke, "Spatially coupled ensembles universally achieve capacity under belief propagation," *IEEE Trans. Inf. Theory*, vol. 59, no. 12, pp. 7761–7813, Dec 2013.
- [18] D. J. Costello, L. Dolecek, T. E. Fuja, J. Kliewer, D. G. M. Mitchell, and R. Smarandache, "Spatially coupled sparse codes on graphs: theory and practice," *IEEE Communications Magazine*, vol. 52, no. 7, pp. 168–176, July 2014.
- [19] D. Guo, Y. Wu, S. S. Shitz, and S. Verdú, "Estimation in Gaussian noise: Properties of the minimum mean-square error," *IEEE Trans. Inf. Theory*, vol. 57, no. 4, pp. 2371–2385, 2011.
- [20] J. Barbier, M. Dia, and N. Macris, "Threshold saturation of spatially coupled sparse superposition codes for all memoryless channels," *Proc. IEEE Inf. Theory Workshop*, 2016.
- [21] Dongning Guo, S. Shamai, and S. Verdú, "Mutual information and minimum mean-square error in Gaussian channels," *IEEE Trans. Inf. Theory*, vol. 51, no. 4, pp. 1261–1282, 2005.
- [22] M. Bayati and A. Montanari, "The dynamics of message passing on dense graphs, with applications to compressed sensing," *IEEE Trans. Inf. Theory*, vol. 57, no. 2, pp. 764–785, Feb. 2011.
- [23] C. Rush and R. Venkataramanan, "The error probability of sparse superposition codes with approximate message passing decoding," *IEEE Trans. Inf. Theory*, vol. 65, no. 5, pp. 3278–3303, May 2019.
- [24] Dongning Guo and S. Verdú, "Randomly spread CDMA: asymptotics via statistical physics," *IEEE Trans. Inf. Theory*, vol. 51, no. 6, pp. 1983–2010, 2005.
- [25] S. Rangan, A. K. Fletcher, and V. K. Goyal, "Asymptotic analysis of MAP estimation via the replica method and applications to compressed sensing," *IEEE Trans. Inf. Theory*, vol. 58, no. 3, pp. 1902–1923, 2012.
- [26] A. Beryhi, R. R. Müller, and H. Schulz-Baldes, "Statistical mechanics of MAP estimation: General replica ansatz," *IEEE Trans. Inf. Theory*, vol. 65, no. 12, pp. 7896–7934, 2019.
- [27] A. Yedla, Y.-Y. Jian, P. S. Nguyen, and H. D. Pfister, "A simple proof of Maxwell saturation for coupled scalar recursions," *IEEE Trans. Inf. Theory*, vol. 60, no. 11, pp. 6943–6965, 2014.
- [28] S. Kudekar, T. J. Richardson, and R. L. Urbanke, "Wave-like solutions of general 1-d spatially coupled systems," *IEEE Trans. Inf. Theory*, vol. 61, no. 8, pp. 4117–4157, 2015.
- [29] J. Barbier, M. Dia, and N. Macris, "Proof of threshold saturation for spatially coupled sparse superposition codes," in *Proc. IEEE Int. Symp. Inf. Theory*, July 2016, pp. 1173–1177.
- [30] A. Javanmard and A. Montanari, "State evolution for general approximate message passing algorithms, with applications to spatial coupling," *Information and Inference: A Journal of the IMA*, vol. 2, no. 2, pp. 115–144, 2013.
- [31] L. Zdeborová and F. Krzakala, "Statistical physics of inference: thresholds and algorithms," *Advances in Physics*, vol. 65, no. 5, pp. 453–552, 2016.